Available online at www.sciencedirect.com

ScienceDirect

Procedia Structural Integrity 81 (2026) 23–30

Structural Integrity Procedia

www.elsevier.com/locate/procedia

VIII International Conference "In-service Damage of Materials: Diagnostics and Prediction" (DMDP 2025)

Effect of geometric imperfections on CO_2 transport pipelines under fatigue loading

Aprianur Fajri[a,b], Nurul Muhayat[a], Ristiyanto Adiputra[c], Aditya Rio Prabowo[a,*], Ben Ganendra[d], Sören Ehlers[e,f], Moritz Braun[e]

[a] Department of Mechanical Engineering, Universitas Sebelas Maret (UNS), Surakarta, Indonesia
[b] Laboratory of Design and Computational Mechanics, Faculty of Engineering, Universitas Sebelas Maret (UNS), Surakarta, Indonesia
[c] Research Center for Hydrodynamics Technology, National Research and Innovation Agency (BRIN), Surabaya, Indonesia
[d] Department of Civil Engineering, Ghent University, Ghent, Belgium
[e] Institute for Maritime Energy Systems, German Aerospace Center (DLR), Geesthacht, Germany
[f] Institute for Ship Structural Design and Analysis, Hamburg University of Technology (TUHH), Hamburg, Germany

Abstract

Catastrophic failures of CO_2 transport pipelines can result in severe economic losses and even casualties. During operation, pipelines are subjected to cyclic loading, which may lead to fatigue failure. The presence of geometric imperfections (GI) arising from installation processes introduces uncertainty that can affect the pipe's strength under these conditions. This study assesses the impact of dent-type GI on the fatigue resistance of CO_2 transport pipelines using a validated finite element method (FEM). Fatigue analysis was conducted using the hot-spot stress approach on the straight tubular pipe with dent-type GI ranging from 0% to 20%. The pipe material is ASTM A36 steel, and the boundary conditions represent an onshore buried pipeline. The results show that the higher the percentage of dent-type GI, the lower the fatigue life due to the stress concentration effect. Further experimental tests and fluid–structure interaction studies are recommended to extend these findings.

Peer-review under responsibility of DMDP 2025 organizers

Keywords: CO_2 transport pipelines; geometric imperfection; dent; finite element method; fatigue analysis

1. Introduction

The concentration of CO_2 in the atmosphere has now exceeded safe limits, contributing to a global temperature increase of more than 1.4 °C above pre-industrial levels. One promising approach to address this issue is carbon capture and storage (CCS) technologies, which capture CO_2 emissions and store them safely (Wennersten et al., 2015). However, this system still faces significant challenges; one of the most critical is the risk of pipeline failure, as pipelines are the primary means of transporting CO_2 . Pipeline failure can result in severe economic losses and even fatalities, particularly in densely populated areas. For instance,

* Corresponding author. Tel.: +62-271-632-163; fax: +62-271-632-163.
E-mail address: aditya@ft.uns.ac.id

2452-3216
Peer-review under responsibility of DMDP 2025 organizers
10.1016/j.prostr.2026.03.005

the 2020 CO_2 pipeline failure in Mississippi, USA, led to 45 reported injuries and damages totaling over US$3.9 million (PHMSA, 2022).

Nomenclatures

k	number of stress levels
n_i	actual number of cycles occurring at the i-th stress level
N_i	number of cycles to failure at the i-th stress level (from the S–N curve)
$\sigma_1, \sigma_2, \sigma_3$	principal stresses (normal stresses along the x, y, and z axes after coordinate rotation, shear stresses = 0)
σ_a, σ_m	stress amplitude and mean stress
σ_e, σ_u	endurance limit and ultimate tensile strength
σ_{eq}	equivalent (von Mises) stress
$\sigma_{max}, \sigma_{min}$	maximum and minimum stress in one cycle

According to the literature, one factor increasing failure risk is geometric imperfections (GI) in the pipeline structure, which reduce its strength under loading (Prabowo et al. (2022); Yasniy et al. (2017); Hanif et al. 2023). Among several types of GI, dent-shaped profiles (Fig. 1) formed during fabrication or installation are believed to have the most significant impact on reducing pipeline strength (Shuai et al., 2020; Ezzati et al., 2021; Dinita, 2023). CCS pipelines are subjected to various loads, including cyclic loads caused by thermal expansion and internal pressure fluctuations. The combination of GI and cyclic loading can lead to fatigue failure. Therefore, accurate prediction and mitigation of this condition are essential to prevent catastrophic events in the future.

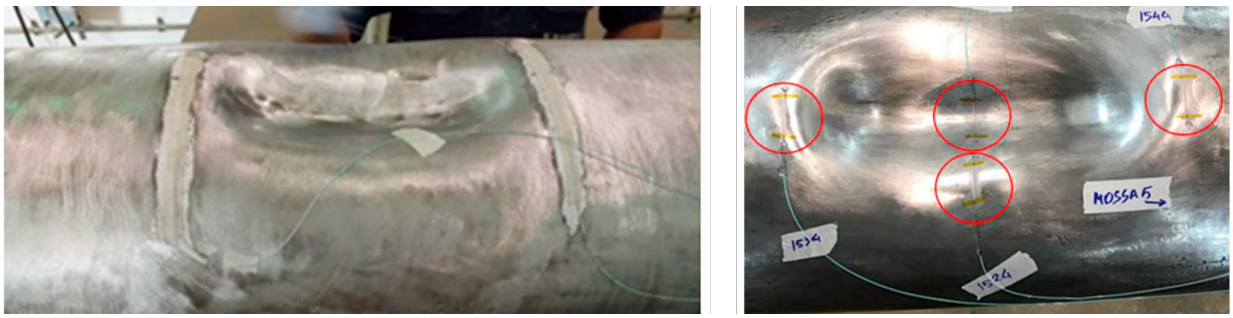

Fig. 1. GI in the form of dents that are suspected to reduce the strength of the pipe structure (Paiva *et al.*, 2021)

2. Fatigue failure on CCS pipelines

Fatigue failure in CCS pipelines usually starts with crack initiation at points with high stress concentration. The location of this crack initiation can be predicted using the stress–life approach (Fajri et al., 2021), based on Finite Element Method (FEM) simulations. In the FEM-based fatigue simulation, the multiaxial stress at each element is converted into a single scalar quantity using the equivalent von Mises stress equation, as shown in Eq. 1. From this scalar stress history, the maximum and minimum stresses in each cycle can be determined to calculate the stress ratio (Eq. 2), as well as the mean stress and stress amplitude. Generally, the S–N curve is obtained from fatigue tests under fully reversed loading conditions ($R = -1$).

However, for actual loading conditions with different stress ratios, a mean-stress correction is required to ensure that the evaluated stress amplitude matches the reference condition of the S–N curve. The Goodman correction theory (Eq. 3) is commonly applied for this purpose, particularly for ductile materials (Pastorcic et al., 2019). Subsequently, the stress cycle history is analyzed using the rainflow counting method to determine the number of cycles at each stress level. Based on the S–N curve, the fatigue life corresponding to each stress level can be estimated. The total fatigue life is then calculated using the Palmgren–Miner rule (Eq. 4), where failure is assumed to occur when the cumulative damage reaches or exceeds one ($D \geq 1$).

$$\sigma_{eq} = \sqrt{\frac{1}{2}[(\sigma_1 - \sigma_2)^2 + (\sigma_2 - \sigma_3)^2 + (\sigma_3 - \sigma_1)^2]} \quad (1)$$

$$R = \frac{\sigma_{min}}{\sigma_{max}} \quad (2)$$

$$\frac{\sigma_a}{\sigma_e} + \frac{\sigma_m}{\sigma_u} = 1 \quad (3)$$

$$D = \sum_{i=1}^{k} \frac{n_i}{N_i} \quad (4)$$

3. Materials and methods

3.1. Research procedure and validation process

In general, this research follows three stages: (1) pre-processing, conducting literature studies to collect reference data and FEM input parameters; (2) processing, validating the FEM model through benchmark analysis and then performing parametric studies on geometry and boundary conditions; (3) post-processing, extracting and analyzing simulation data to interpret the observed phenomena. The validation process was carried out by re-simulating the study by Köksal *et al,* (2013). The resulting error was less than 5% (Fig. 2), indicating that our FEM approach is valid and reliable

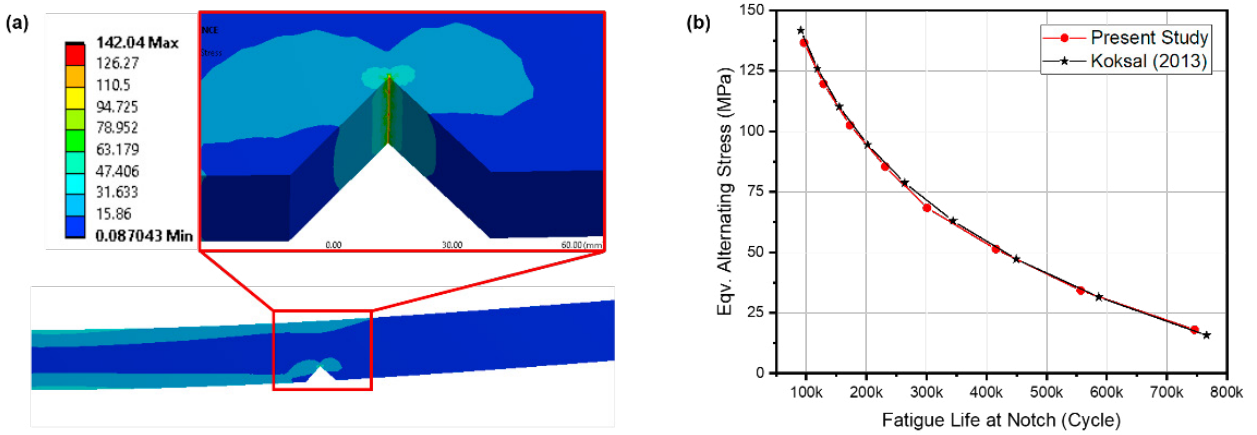

Fig. 2. Validation of the method used: (a) stress distribution contour, and (b) benchmark analysis.

3.2. Material and geometry modelling

The material used in this study is ASTM A36 steel, with its mechanical properties shown in Table 1 and its S-N curve from the uniaxial fatigue test shown in Fig. 3a. The pipeline model has a length of 5,000 mm, an outer diameter of 300 mm, and a wall thickness of 10 mm. This geometry has a slenderness ratio of < 50, which is very suitable for observing local failure phenomena. The dent imperfection ranged from 0% to 20% of the pipe diameter. Details of the model configuration and loading type are presented in Table 2 and Fig. 3b.

Table 1. Material properties of ASTM A36 steel.

Yield tensile strength (MPa)	Ultimate tensile strength (MPa)	Elastic modulus (GPa)	Poisson's ratio	Elongation at break (%)	Corrected endurance limit (MPa)
250	460	200	0.3	18	195

Table 2. Model configuration.

Sample	%Dent ($\frac{d_p}{D_e} \times 100\%$)	Dimension ($length;\ D_e; t$)	Slenderness ratio (λ)	Load
Geometry 1	0	5,000; 300; 10 mm	48.8	Type 1, Type 2
Geometry 2	5			
Geometry 3	10			
Geometry 4	15			
Geometry 5	20			

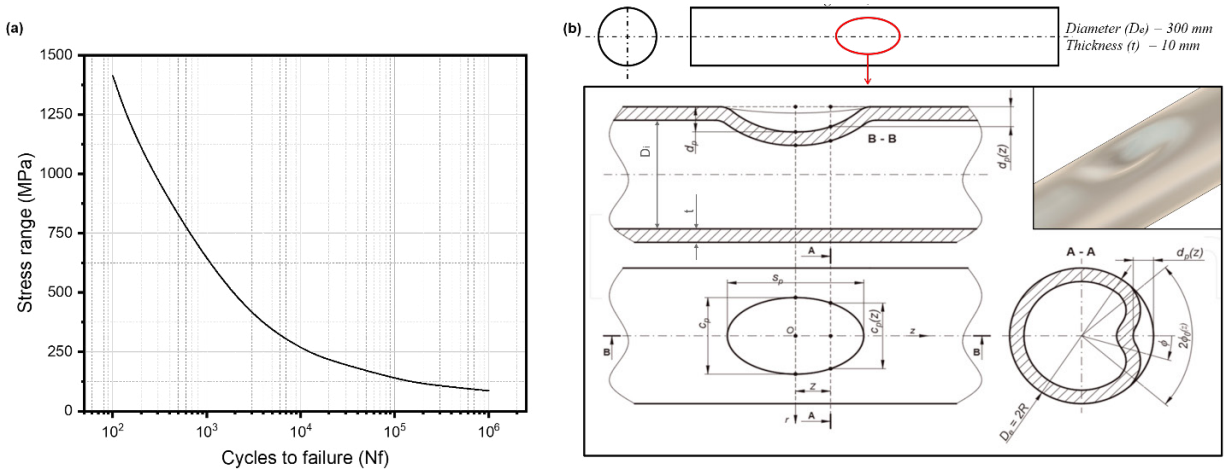

Fig. 3. (a) S-N curve of ASTM A36 steel, adapted from Gorash and MacKenzie, (2017); and (b) geometry model, adapted from Dinita, (2023).

3.3. Meshing strategy and boundary condition

In this study, a hexahedral mesh was used to generate solid elements (Fig. 4a). At the initial stage, several mesh size variations were applied to the model geometry. A simple static analysis was then performed to assess mesh independence. One end of the pipe was fixed, while a lateral load was applied at the opposite end. The maximum hot-spot stress in the dent region and the corresponding computational time were recorded and plotted to generate the convergence curve. The mesh convergence analysis showed that element aspect ratios between 2 and 4 gave the best compromise between accuracy and computational time (Fig. 4b). Based on that analysis, a mesh size of 40 mm was determined to be optimal for this study, as it has an aspect ratio of 4. When applied to the geometry, the 40 mm mesh size generates 3,800 elements and has a relatively light computational load.

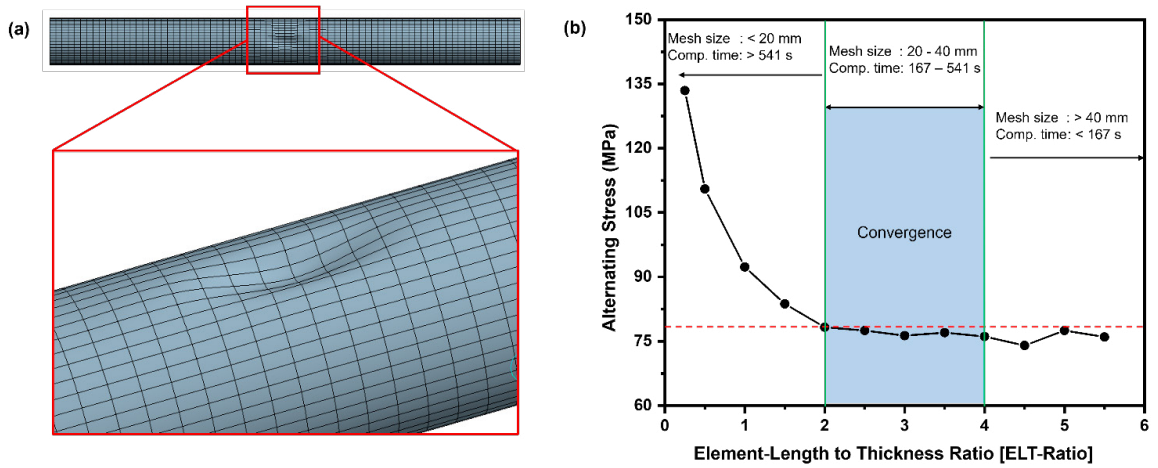

Fig. 4. Meshing procedure: (a) mesh convergence test; (b) hexahedral mesh

The boundary conditions define the direction and location of applied loads (Fig. 5). Two loading types were simulated to represent real field conditions, both in axial and radial directions. Fixed supports and displacement control were applied to account for the soil resistance surrounding the buried pipeline. Load type 1 corresponds to an axial load acting along the pipeline axis. An axial cyclic force (F) of ±500 kN was applied to each model, producing different alternating hot-spot stress levels depending on the dent depth variation. These alternating hot-spot stress values were subsequently adopted for the fatigue analysis. Load type 2 represents a cyclic internal pressure (P) of ±3.5 MPa. Similar to load type 1, cyclic internal pressure induces alternating stress in the dented region. The resulting alternating stress values were likewise used in the fatigue assessment. Both loading cases correspond to a fully reversed condition ($R = -1$); therefore, the stress amplitude is equal to the maximum stress within a single cycle ($\sigma_a = \sigma_{max}$). Loading was applied continuously until crack initiation in the pipe. The number of cycles to crack initiation was taken as a measure of the pipe's fatigue life.

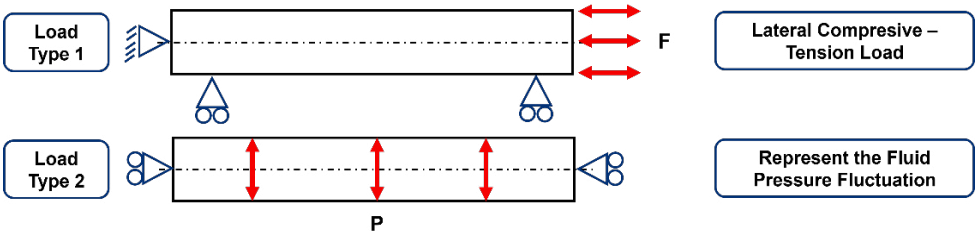

Fig. 5. Boundary conditions for the finite element analysis.

4. Result and discussion

After all the numerical simulations were completed, contour figures were generated to represent the distribution of each parameter. These figures were then extracted and analyzed together with quantitative data to explain the characteristics of the pipe model under cyclic loading

4.1. Alternating stress distribution

The numerical simulation results show that the pipe without GI experiences alternating stress with a relatively uniform distribution under load type 1 (Fig. 6). The maximum alternating stress is approximately 60.34 MPa, which is well below the endurance limit. This condition indicates that the pipe operates safely in accordance with the applicable design criteria. However, when the GI is introduced, the stress distribution changes significantly. A noticeable stress concentration occurs in the GI region, accompanied by a gradual increase in the maximum alternating stress to 78.27 MPa, 84.6 MPa, 97.02 MPa, and 112.26 MPa at dent levels of 5%, 10%, 15%, and 20%, respectively.

A similar pattern is observed under load type 2, which represents fluid pressure fluctuations. Under this condition, the alternating stress in the dented area increases significantly. For a pipe without a dent, the maximum alternating stress is 16.34 MPa with a relatively uniform distribution. However, when a 5% dent is present, the maximum alternating stress rises sharply to 190.47 MPa, accompanied by stress concentration around the dented area. The maximum alternating stress continues to increase with increasing dent depth, reaching 298.9 MPa at a 20% dent level. Compared to the material's endurance limit, a 10% dent is already considered unsafe, as it produces an alternating stress exceeding the endurance limit. These findings are consistent with ASME standards, which recommend limiting dent deformation to a maximum of 6% to maintain the structural integrity of the pipe (ASME, 2003).

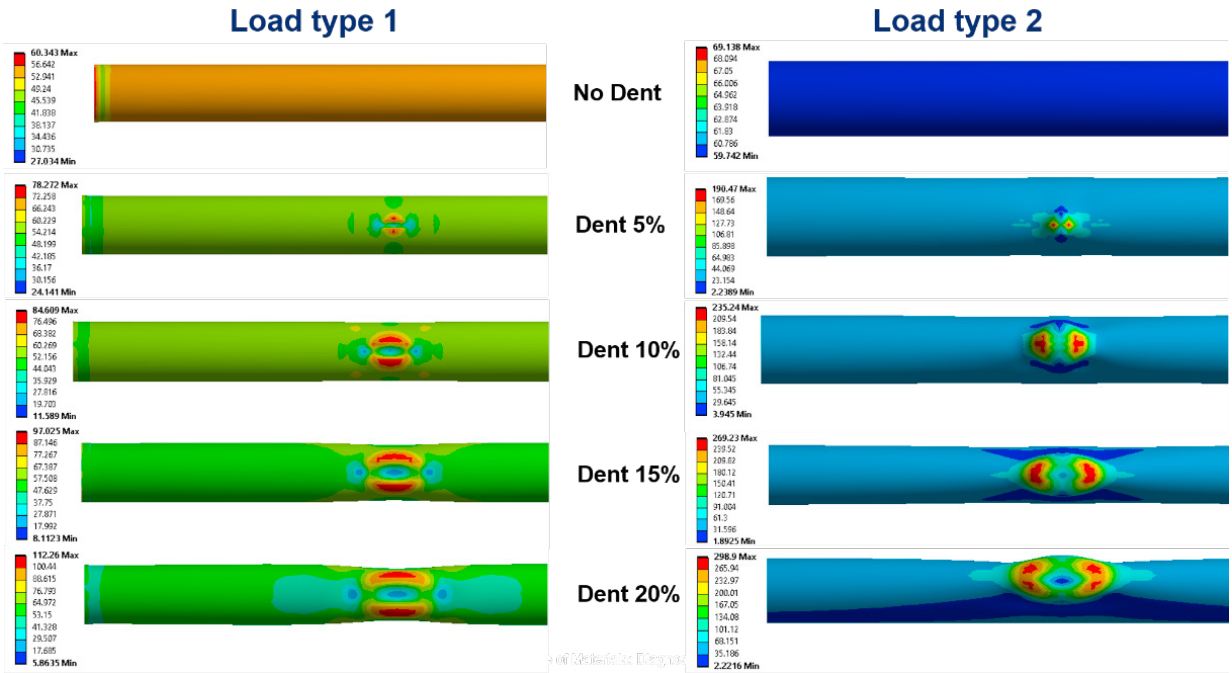

Fig. 6. FEM result: alternating stress under load types 1 and 2.

4.2. Biaxiality indication

Fig. 7 illustrates the changes in direction and principal stress components due to the presence of GI, as indicated by the biaxiality. A value of 0 represents a uniaxial condition, while a value of ±1 indicates a multiaxial condition. It can be observed that both load types 1 and 2 tend to produce multiaxial stress on the dent profile, which is not uniformly distributed. This condition will affect the model's behavior under fatigue loading.

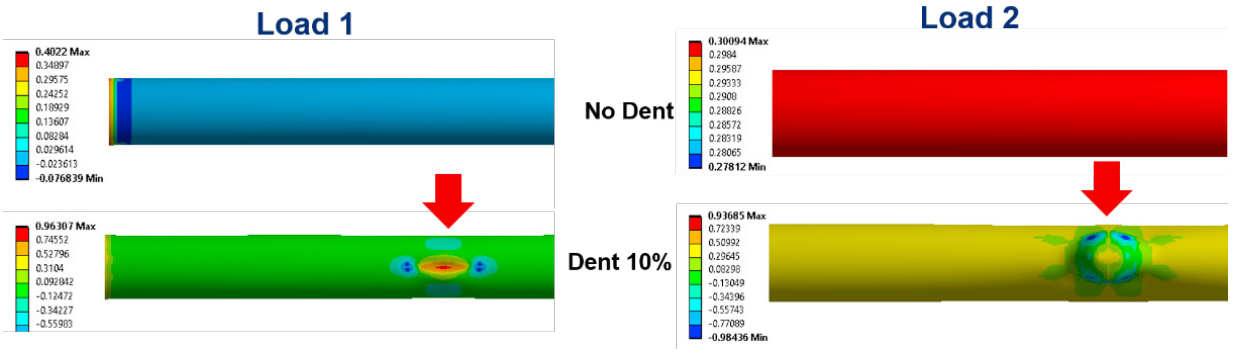

Fig. 7. FEM result: biaxiality indication.

4.3. Fatigue life

Fig. 8 illustrates the effect of stress concentration on the pipeline's fatigue life. The analysis results indicate that the normal pipeline subjected to both load types 1 and 2 remains within the safe operating range and can withstand more than 1 million loading cycles. However, the minimum fatigue life in the critical region decreases with increasing GI percentage. Moreover, Fig. 9 shows that load type 2 poses a higher risk to the pipeline's structural integrity than load type 1.

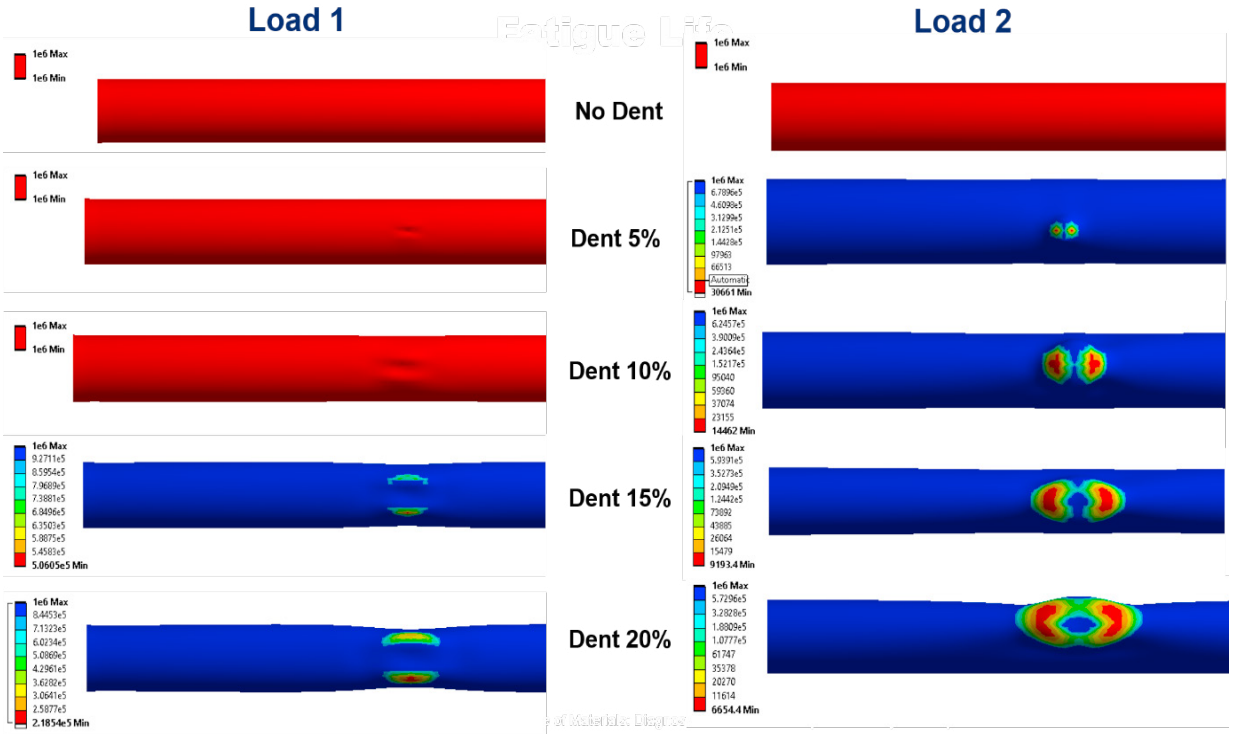

Fig. 8. FEM result: fatigue life.

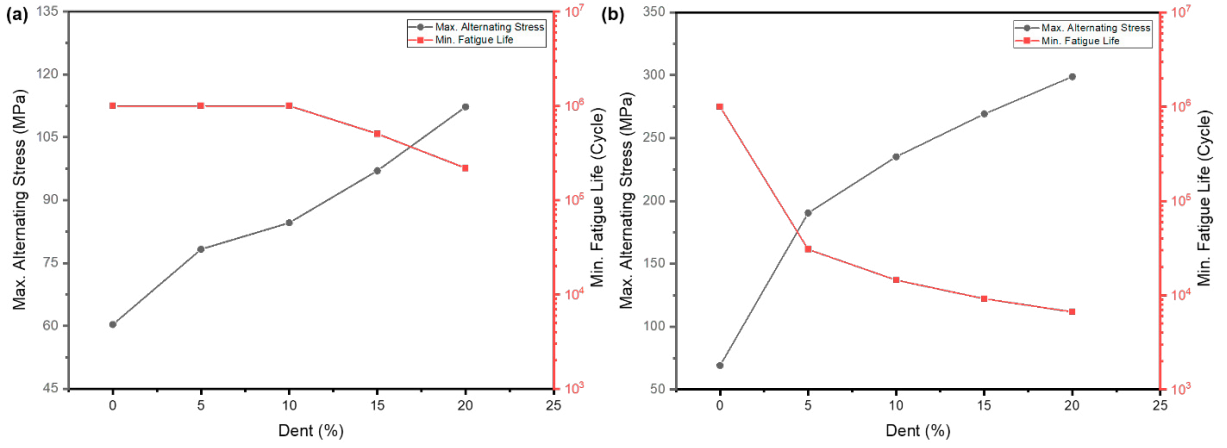

Fig. 9. Stress result vs fatigue life; (a) load type 1; and (b) load type 2.

4.4. Fatigue safety factor

Fig. 10 presents the analysis of the safety factor (SF) against fatigue for a design life of one million cycles. Unlike in static loading conditions, an SF $\geqslant 1$ in fatigue analysis is considered safe. As shown in Fig. 10, a 5% dent significantly increases the likelihood of fatigue failure, particularly under load type 2. Meanwhile, a 10% dent remains within the safe range under load type 1, but may lead to structural failure after only a few thousand cycles under load type 2.

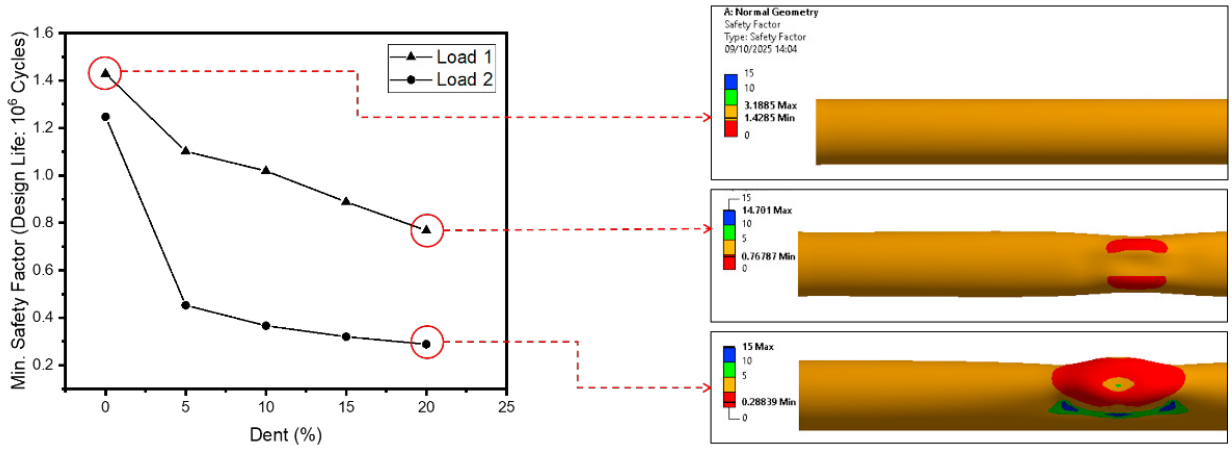

Fig. 10. Fatigue safety factor for 10^6-cycle design life.

5. Concluding remarks

The effect of GI on the fatigue strength of CO_2 transportation pipelines has been studied. The results show that dent-shaped GI significantly reduces the fatigue life of the modeled pipe structure. The dent profile alters the effective cross-sectional area, thereby inducing stress concentration. This stress concentration is the primary cause of crack formation after undergoing a specific loading cycle. From a loading perspective, fluctuating internal pressure in type 2 is more hazardous and requires greater attention than loading in type 1. For further research, this result needs to be validated using experimental methods or numerical modeling of fluid-structure interaction to provide a more comprehensive picture.

Acknowledgements

This research was funded by the Indonesia Endowment Fund for Education (LPDP), Ministry of Finance, Republic of Indonesia.

References

ASME, 2003. ASME B31.8: Gas Transmission and Distribution Piping Systems. American Society of Mechanical Engineers, New York, United States.

Dinita, A., 2023. Assessment of the Structural Integrity of the Pipes with Anomalies Such as Local Elastic-plastic Deformations, in: Pipeline Engineering - Design, Failure, and Management. IntechOpen, pp. 1–16.

Ezzati, M., Naghipour, M., Zeinoddini, M., Zandi, A.P., Elyasi, M., 2021. Strain ratcheting failure of dented steel submarine pipes under combined internal pressure and asymmetric inelastic cycling. Ocean Engineering, 219, 108336.

Fajri, A., Prabowo, A.R., Muhayat, N., Smaradhana, D.F., Bahatmaka, A., 2021. Fatigue Analysis of Engineering Structures: State of Development and Achievement. Procedia Structural Integrity, 33, 19–26.

Gorash, Y., MacKenzie, D., 2017. On cyclic yield strength in definition of limits for characterisation of fatigue and creep behaviour. Open Engineering, 7, 126–140.

Hanif, M.I., Adiputra, R., Prabowo, A.R., Yamada, Y., Firdaus, N., 2023. Assessment of the ultimate strength of stiffened panels of ships considering uncertainties in geometrical aspects: Finite element approach and simplified formula. Ocean Engineering, 286, 115522.

Köksal, N.S., Kayapunar, A., Cevik, M., 2013. Fatigue Analysis of a Notched Cantilever Beam using Ansys Workbench. Proceedings of the Fourth International Conference on Mathematical and Computational Applications, 111–118.

Paiva, V., Gonzáles, G., Vieira, R., Ribeiro, A., Maneschy, J., Diniz, J., D'Almeida, A., Freire, J., 2021. Fatigue Tests on Buried or Repaired Dented Steel Pipeline Specimens. Metals, 11(12), 2031.

Pastorcic, D., Vukelic, G., Bozic, Z., 2019. Coil spring failure and fatigue analysis. Engineering Failure Analysis, 99, 310–318.

PHMSA, 2022. Failure Investigation Report – Denbury Gulf Coast Pipelines LLC Pipeline Rupture/ Natural Force Damage. Pipeline and Hazardous Materials Safety Administration, New Jersey, United States.

Prabowo, A.R., Ridwan, R., Tuswan, T., Imaduddin, F., 2022. Forecasting the Effects of Failure Criteria in Assessing Ship Structural Damage Modes. Civil Engineering Journal, 8(10), 2053-2068.

Shuai, Y., Zhou, D.C., Wang, X.H., Yin, H.G., Zhu, S., Li, J., Cheng, Y.F., 2020. Local buckling failure analysis of high strength pipelines containing a plain dent under bending moment. Journal of Natural Gas Science and Engineering, 77, 103266.

Wennersten, R., Sun, Q., Li, H., 2015. The future potential for Carbon Capture and Storage in climate change mitigation – an overview from perspectives of technology, economy and risk. Journal of Cleaner Production, 103, 724–736.

Yasniy O., Pyndus Yu., Iasnii V., Lapusta Y., 2017. Residual lifetime assessment of thermal power plant superheater header. Engineering Failure Analysis 82, 390-403.